



## Production of electricity by photoelectrochemical oxidation of ethanol in a PhotoFuelCell

Maria Antoniadou, Panagiotis Lianos\*

University of Patras, Engineering Science Dept., 26500 Patras, Greece

### ARTICLE INFO

#### Article history:

Received 2 May 2010

Received in revised form 21 June 2010

Accepted 23 June 2010

Available online 30 June 2010

#### Keywords:

Photoelectrochemical cell

Ethanol photocatalytic oxidation

PhotoFuelCell

### ABSTRACT

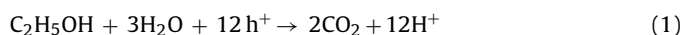
Photocatalytic oxidation of ethanol was carried out in a non-biased photoelectrochemical cell at high pH. The cell was made of two compartments separated by a silica frit, both filled with aerated NaOH electrolyte. The anode electrode bore multilayer nanocrystalline titania, made of either commercial Degussa P25, sol–gel synthesized titania or both. The cathode electrode was made of carbon cloth carrying Carbon Black and Pt as catalyst. When the anode was excited by UVA radiation (363 nm), the cell produced electricity very efficiently. The open-circuit voltage was 0.88 V in the absence and almost 1.2 V in the presence of ethanol. The current increased by more than an order of magnitude by adding ethanol, showing that it is much more efficient to oxidize ethanol than to oxidize (split) water. The performance of the cell improved when a compact titania layer was introduced between the FTO electrode and the thick photocatalytic layer. Ethanol was used as a model fuel but the cell can run on many other organic substances as well. The cell can be used as a source of renewable electricity, by consuming organic wastes under photo-excitation, thus making a PhotoFuelCell.

© 2010 Elsevier B.V. All rights reserved.

### 1. Introduction

Conversion of solar energy to electricity is mainly realized using photovoltaic cells. However, it is possible to produce electricity photoelectrochemically with simultaneous photodegradation of organic wastes in the presence of photocatalysts. In that case, a double environmental benefit is made, that is, renewable electricity is produced and waste material is consumed. This idea is not new. Photocatalytic degradation of organic substances is being studied for several decades with the purpose to produce renewable hydrogen using solar light [1–16]. After the discovery that oxide semiconductors can be employed as photoanodes in photoelectrochemical (PEC) cells to split water, a tremendous interest in such systems has arisen [17–27]. In the original works, single crystals [17], hot pressed polycrystalline electrodes [18], or even suspended particles [19] have been employed but with limited efficiency. Nowadays, easy handling of nanocrystalline semiconductors and the availability of new materials and processes has given a new impulse and created new strong interest in these systems. Photoelectrochemical water splitting and production of hydrogen using solar radiation is indeed an exciting subject of research. However, it is much more efficient to photoelectrochemically oxidize an organic substance and produce hydrogen than to split water

[28,29]. The idea is the following: when a semiconductor photocatalyst absorbs photons, electron–hole pairs are created. Holes oxidize the photodegradable substance, either directly or through  $\text{OH}^-$  intermediates. Indeed  $\text{OH}^-$  scavenge holes and give reactive  $\text{OH}^\cdot$  radicals with strong oxidative power. Oxidation of the organic substance (or water itself) may liberate hydrogen ions, which diffuse in the solution. The overall reaction for hydrogen generation, for example, in the case of ethanol (cf. Ref. [1]) is as follows:



The concentration of hydrogen ions in solution depends on the presence of hydroxyl ions, since the latter interact with hydrogen ions producing water:



Combination of reactions (1) and (2) gives the following reaction (3), valid in basic environments, which is the most usual case:



On the other hand, the fate of electrons depends on the applied conditions. If the semiconductor photocatalyst is deposited on an electrode (the anode), which is externally connected to a counter electrode (the cathode), and if the cathode potential, at open-circuit conditions, is positive enough with respect to that of the conduction band of the semiconductor, electrons are channeled away from the semiconductor towards the cathode. There, they can participate in reductive interactions. Thus in the absence of oxygen they reduce

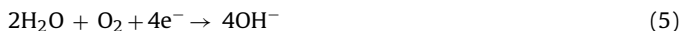
\* Corresponding author. Tel.: +30 2610 997513; fax: +30 2610 997803.

E-mail address: [lianos@upatras.gr](mailto:lianos@upatras.gr) (P. Lianos).

water generating molecular hydrogen:



while in the presence of oxygen they give



Both cases lead to  $\text{OH}^-$  regeneration feeding the system in a cyclic manner. Thus hydroxyl ions are consumed during oxidation and they are regenerated during reduction. The present work studies interactions in the presence of oxygen.

A PEC cell consuming an organic substance (the “Fuel”) producing electricity under photo-excitation is a PhotoFuelCell (PFC) [30,31]. This term was previously introduced by Kaneko et al. [30]. A PFC is in many ways more interesting than a fuel cell. Take, for example, a methanol fuel cell. Such a cell necessitates the use of a costly anode, made of noble metals plus elevated temperature (about 50–120 °C), in order to split methanol. A PFC splits fuel using light and a semiconductor photocatalyst, which is much easier and less costly to make and to operate. In addition, a photocatalyst works at ambient conditions, has no selectivity and can degrade potentially any organic substance, be it a product of biomass or a water waste. Furthermore, the semiconductor photocatalyst can function in aqueous media with only limitation the necessity for light to reach the photocatalyst. Thus it can work even with high pollutant loads, if it is deposited on a transparent electrode, using back side excitation.

The function of any photoelectrochemical cell depends on whether there is sufficient bias to drive electrons from the anode to the cathode. The potential of the cathode in an acidic environment and in the absence of oxygen is equal to that of the  $\text{H}^+/\text{H}_2$  level, which is close to zero. When the anode is made of titania, the potential difference is too small to drive electrons. Indeed, the conduction band of this semiconductor is about  $-0.2\text{ V}$  and this is not strong enough potential difference. Thus in that case, the current is practically zero. In the presence of oxygen, the cathode actually acts as an oxygen electrode ( $\text{H}_2\text{O}/\text{O}_2$ ) [18]. The level of an oxygen electrode should theoretically be at  $+1.23\text{ V}$  but in practice it appears around  $+0.8\text{ V}$  [18]. The reason for this drop is due to various non-identified losses and mainly to the mixture of the following two redox levels:  $\text{O}_2 + 4\text{H}^+ + 4\text{e}^- \rightarrow 2\text{H}_2\text{O}$  ( $+1.23\text{ V}$ ) and  $\text{O}_2 + 2\text{H}^+ + 2\text{e}^- \rightarrow \text{H}_2\text{O}_2$  ( $+0.682\text{ V}$ ) [32]. Thus in the presence of oxygen, there exists enough driving force and indeed a substantial electric current is observed. Since sufficient potential difference between anode and cathode is then necessary, various techniques have been devised to obtain it. If the cell is divided into two compartments, separated by an ion transfer membrane, then it is possible to use two different electrolytes of different pH values in the two compartments [28,29]. It is known that in that case an additional (chemical) bias can be applied, which is given by [22]:

$$\Delta E = 0.059 \times \Delta \text{pH} (\text{Volts}) \quad (6)$$

Further additional bias is obtained by adding fuel in the anode compartment, as it will be discussed later. In our previous works [28,29,33] we have studied two-compartment cells using a basic electrolyte in the anode compartment and an acidic electrolyte in the cathode compartment. The strong chemical bias applied in that case led to high values of open-circuit voltage. The compartments were separated by a nafion membrane. Such cells are good for research laboratory work but they are rather impractical for industrial applications. In addition to the costly reagents, nafion membranes cannot sustain a long time operation since both alkali and hydrogen ions pass through the membrane and modify the original conditions. With this in mind, in the present work we studied PhotoFuelCells without chemical bias and searched for optimized conditions offering sufficient conversion efficiencies.

## 2. Experimental

### 2.1. Materials

Unless otherwise indicated, reagents were obtained from Aldrich and were used as received. The nanocrystalline titania was either commercial Degussa P25 or it was synthesized by the sol-gel process using Titanium Tetraisopropoxide (TTIP) as precursor. Millipore water was used in all experiments.  $\text{SnO}_2:\text{F}$  transparent conductive electrodes (FTO, Resistance  $8\ \Omega/\square$ ) were purchased from Pilkington, USA. Carbon cloth, 20% wet proofing and Pt/Carbon Black electrocatalyst (30% on Vulcan XC72) were purchased from BASF Fuel Cell, Inc., USA. Carbon Black, Vulcan XC72R, was a gift from CABOT Corporation.

### 2.2. Preparation of the anode

Most of the anode electrodes were based on commercial titania. Degussa P25 was applied on FTO electrodes using a home-made paste, which was prepared according to the recipe given in Ref. [34]. Two layers of titania were applied giving a uniform film of about 8–10  $\mu\text{m}$  thick. An image of such a film can be seen in Ref. [35] and will be also described later. The film was calcined at 550 °C. The active surface of each titania film was  $3 \times 4 = 12\text{ cm}^2$ . A picture of a similar electrode can be seen in Ref. [33]. Electric conduct was made using an adhesive copper ribbon and a copper wire soldered on the copper ribbon. Sol-gel titania was deposited by the following procedure [35]: 1.4 g of the non-ionic surfactant Triton X-100 was mixed with 7.6 ml ethanol. Then we added 1.36 ml glacial acetic acid ( $\text{AcOH}$ ) and 0.72 ml of TTIP under vigorous stirring. After a few minutes stirring, the film was deposited on the FTO electrode by dipping and then it was dried for a few minutes at 80–100 °C. Subsequently, a second layer was deposited also by dipping. Finally, it was calcined for 10 min at 550 °C with a temperature ramp of 20 degrees/min. The thus obtained 2-layer film had a thickness of about 500 nm, as it will be discussed later. Thicker films could be obtained by depositing more layers by exactly following the above procedure. This sol-gel deposited film was a transparent material, even at multiple layers.

### 2.3. Preparation of the cathode

Special care was taken for the construction of the cathode electrode, in order to increase its efficiency. Cathode was made of carbon cloth with deposited Carbon Black and Pt as described in a previous publication [31]. An amount of 0.246 g of Carbon Black was mixed with 8 ml of distilled water by vigorous mixing in a mixer (about 2400 r.p.m.) until it became a viscous paste. This paste was further mixed with 0.088 ml polytetrafluorethylene (Aldrich, Teflon 60 wt.% dispersion in water) and then applied on a carbon cloth cut in the necessary dimensions. This has been achieved by first spreading the paste with a spatula, preheating at 80 °C and finally heating in an oven at 340 °C. Subsequently, the catalytic layer was prepared as follows: 1 g of Pt/Carbon Black electrocatalyst (30% on Vulcan XC72) was mixed with 8 g of Nafion perfluorinated resin (5 wt. % solution in lower aliphatic alcohols and water, Aldrich) and 15 g of a solution made of 7.5 g  $\text{H}_2\text{O}$  and 7.5 g isopropanol. The mixture was ultrasonically homogenized and then applied on the previously prepared carbon cloth bearing Carbon Black. Then the electrode was heated at 80 °C for 30 min and the procedure was repeated as many times as necessary to load about 0.5 mg of Pt/ $\text{cm}^2$ . The thus prepared Pt/carbon cloth (Pt/CC) electrode was ready for use. Its size was similar to the anode electrode, i.e.  $3 \times 4 = 12\text{ cm}^2$ .

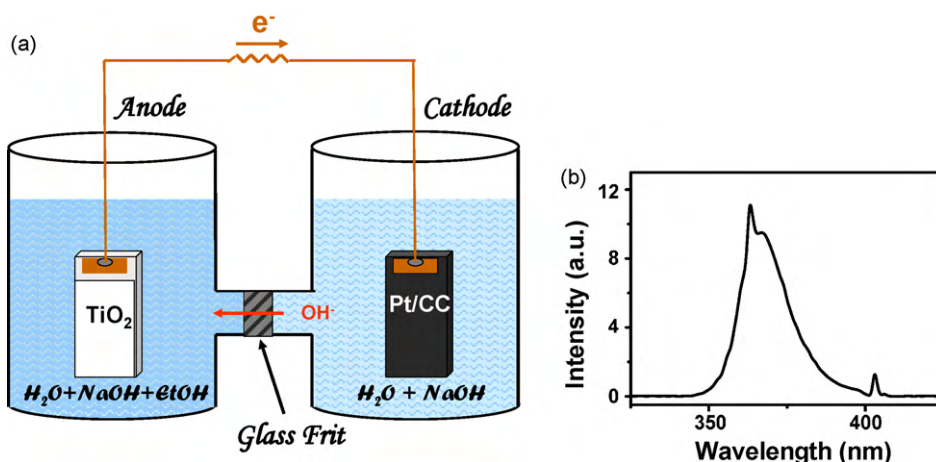


**Fig. 1.** (a) Schematic representation of the two-compartment reactor. The anode compartment contained 150 ml of an aqueous solution of ethanol at various concentrations and 1 M NaOH. The cathode compartment contained the same electrolyte as the anode compartment but without alcohol. Diffusion of  $\text{OH}^-$  ions is expected from the cathode to the anode compartment through the glass frit. (b) Spectral profile of the Light source (Black Light).

#### 2.4. Description of the reactor

The reactor was made of pyrex glass of cylindrical shape (55 mm internal diameter). We used two types of reactor. One-compartment reactor was just a cylindrical tube about 10 cm long. Two-compartment reactor had an H shape. The two compartments were separated by a silica frit (ROBU, Germany, porosity SGQ 5, diameter 25 mm, thickness 2 mm). In all cases, the compartments could be tightly capped with pyrex fittings having provisions for electrode connections and gas inlet–outlet. However, in most cases they were open to the ambient. Each compartment could carry about 150 ml of electrolyte. The electrolyte was an aqueous solution of NaOH at various concentrations ranging from 0.1 to 1.0 M. A schematic representation of the reactor is given in Fig. 1a. As fuel we used ethanol. The cell could work with many other substances but ethanol was presently used as a model fuel. UVA excitation of titania was made using Black Light fluorescent tubes, peaking around 363 nm (Fig. 1b). Four tubes, each of 4W nominal power, were placed around the anode compartment (or the single-compartment cell) and they were covered by a cylindrical protecting–reflecting cover, having a slot that allowed the cathode compartment to be placed outside the lamp system in the dark. This reactor and excitation source configuration was very convenient for the present application, since it was not sensitive to sample direction or position in the cavity. The total radiation intensity incident on the sample was estimated to be around  $3.5 \text{ mW/cm}^2$ .

#### 2.5. Apparatus

Electrochemical measurements were carried out with an Autolab potentiostat PGSTAT128N. All current–voltage curves were traced at  $20 \text{ mV/s}$ . Radiation intensity was measured with a PMA 2100 Radiant Power meter (Solar Light Co.), calibrated for the Near UV spectral range. FESEM (Field Emission Scanning Electron Microscopy) images were obtained with a Zeiss SUPRA 35VP microscope.

### 3. Results and discussion

The purpose of the present work, as already said, was to construct and to optimize a PhotoFuelCell (PFC) that consumes a fuel under photocatalytic conditions and produces electricity. This cell can run potentially with any organic substance as a fuel. However, in the present work, ethanol was used as a model fuel, since it is

simple and efficient, as shown in our previous works [28,29]. PFC must be filled with an electrolyte, which determines the internal (ionic) conductivity of the cell. A basic electrolyte has been used, namely NaOH. The reason is that titania photocatalyst works more efficiently in basic environments thanks to the presence of  $\text{OH}^-$  ions, which act as hole scavengers thus preventing electron–hole recombination and facilitating the oxidation process. The concentration of NaOH was optimized in separate experiments. It was concluded to use 0.2 M in the case of the single-compartment cell operating with a three-electrode system while for the self-sustained non-biased two-compartment cell, the concentration was 1 M.

#### 3.1. IV characteristics of a single-compartment cell employing a three-electrode system. Effect of ethanol on photocurrent

A titania electrode made of two layers of Degussa P25, as described above, was used as working electrode and Pt/CC as counter electrode, while a Ag/AgCl electrode was used as reference. Fig. 2 shows current–voltage characteristics under illumination and in the dark, in the absence and in the presence of ethanol.

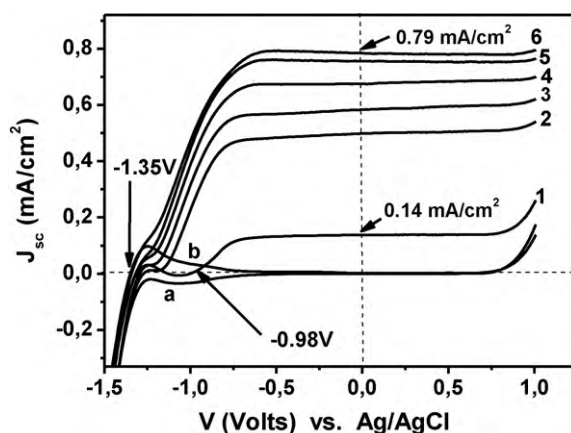


**Fig. 2.** Variation of current density with voltage in a three-electrode single-compartment reactor. Curves 1–6 were recorded under UVA (Black Light) irradiation and correspond to various ethanol volume percentages: (1) 0, (2) 0.1, (3) 1.0, (4) 5, (5) 10, and (6) 20. Curves (a) and (b) were recorded in the dark: (a) in the absence of ethanol and (b) in the presence of 20 vol.% ethanol. The electrolyte contained 0.2 M NaOH. The values of the actual currents measured can be calculated by multiplying by  $12 \text{ cm}^2$  (the surface of the anode electrode).



The dark current was practically zero. The saturation current in the absence of ethanol was 1.7 mA (0.14 mA/cm<sup>2</sup>) but a small quantity of ethanol in the solution, i.e. 0.1 vol.% (0.014 M) raised current by a factor larger than 3. Further addition of ethanol always increased current but the increase was slower at higher ethanol concentrations. The increase of the photocurrent in the presence of ethanol is due to the efficient trapping of holes, as it becomes obvious from reaction (3). Indeed, it takes one molecule of ethanol to retain 12 h<sup>+</sup> (12 holes). Of course, the larger the number of charge carriers, the more difficult is to realize a reaction. However, reaction (3) describes an overall scheme. In reality, this reaction is realized in many steps with one or two holes involved in each step [1,6,7]. Such steps are favored, because the Gibbs free energy change during each step is small. For example, the first step of ethanol photocatalytic oxidation, i.e.  $C_2H_5OH \rightarrow CH_3CHO + H_2$ , involves a Gibbs free energy change of 40.8 kJ/mol [1], while the corresponding value for oxidation of water, i.e.  $H_2O \rightarrow H_2 + 1/2O_2$ , is 237.14 kJ/mol [11].

Similar differences are measured for other steps [1] as well as for other alcohols [9]. For several years, authors supported the theory of “current doubling” in the presence of photocatalytically oxidized species [21,36,37]. Current doubling has indeed been observed in the photocatalytic oxidation of alcohols and other organic sacrificial agents using ZnO but also TiO<sub>2</sub> photocatalysts [21]. Current doubling is due to two-step photocatalytic oxidation. In the first step, an oxidized radical intermediate is formed by interaction with one hole. Then the radical injects an electron in the conduction band of the semiconductor photocatalyst while it reaches its final oxidized state. Thus for one photon absorbed, two electrons are created in the conduction band, one by electron–hole dissociation and one by injection from the radical species; hence the observed current is doubled. Some authors observed a current multiplication and ascribed it to the particularity and the specificity of the employed photocatalyst [38,39]. Current multiplication is, however, a more general phenomenon. Indeed, Fig. 2 shows that current is multiplied several times in the presence of ethanol. We believe that current doubling may be incorporated in the above current values but the obtained values of Fig. 2 simply demonstrate the large capacity of ethanol to act as a sacrificial agent leading to efficient hole retaining and effective electron–hole separation. Thus it is much more efficient to oxidize ethanol than to oxidize water.

Another important feature of Fig. 2 is the difference in the open-circuit voltage (voltage at zero current) in the presence as compared to the absence of ethanol. Even though, the exact difference is obscured by the interference of the anodic peak around −1.3 V, a difference of about 0.3 V is expected in the presence of ethanol, which indicates the higher reactivity of ethanol. This additional 0.3 V is added to the anodic potential thus increasing current flow, as it will be discussed later.

### 3.2. The PhotoFuelCell. A self-sustained non-biased two-compartment cell

As mentioned in Section 1, when the cathode functions as an oxygen electrode, i.e. when the electrolyte is aerated, it is placed at a potential of about +0.8 V. Since the potential of titania conduction band is around −0.2 V, a higher potential difference of +0.8 V is expected for a cell functioning with a titania anode. The above values correspond to acidic pH. When a basic electrolyte is used, both the cathode potential and the semiconductor potential are raised by the same amount [22]; therefore, the above potential difference should be preserved. Indeed, a two-compartment cell was constructed, as explained in Section 2, and it was filled with water containing 1.0 M NaOH, both in the anode and in the cathode compartment. A silica frit was used as an ion transport membrane. The

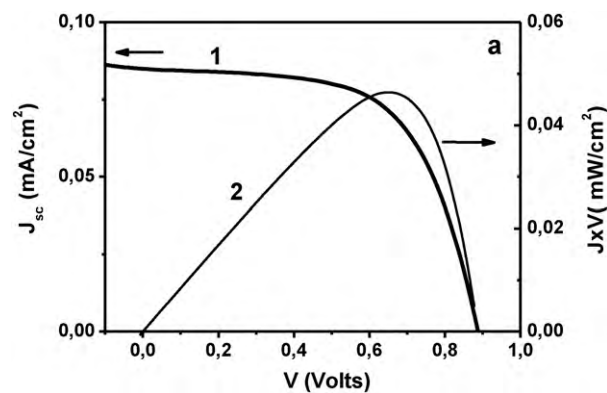


Fig. 3. JV curve (1) and variation of the  $J \times V$  product (2) for a cell without ethanol. The corresponding fill factor was 0.61. The electrolyte was 1 M NaOH. Excitation at 363 nm using a Black Light source.

anode was the above described titania electrode and the cathode the Pt/CC electrode. Measurement of current–voltage characteristics of this cell was made by drawing curves, as the one of Fig. 3. The open-circuit voltage of the cell was 0.88 V, which is within the expected range. The current density in Fig. 3 was obtained by dividing the measured current by the active surface of the anode, i.e. 12 cm<sup>2</sup>. This cell had a good fill factor, i.e. 0.61. The fill factor (FF) was calculated by the formula:  $FF = (JV)_{\max} / J_{sc} V_{oc}$ , where  $J_{sc}$  is the short-circuit current density and  $V_{oc}$  the open-circuit voltage (0.085 mA/cm<sup>2</sup> and 0.88 V, respectively, in the case of Fig. 3).  $(JV)_{\max}$  is the maximum value of the  $J \times V$  product, the values of which are depicted by curve (2) in Fig. 3.  $(JV)_{\max}$  was equal to 0.046 mW/cm<sup>2</sup>, therefore,  $FF = 0.61$ . Since excitation of titania was made with a practically monochromatic source (Fig. 1b), the performance of the cell can be appreciated by its External Quantum Efficiency, which can be measured by the Incident Photon to Charge carrier Efficiency (IPCE, expressed in %) [40]:

$$IPCE\% = \frac{1240 \times J_{sc}(\text{mA/cm}^2)}{\lambda(\text{nm}) \times P(\text{mW/cm}^2)} \times 100 \quad (7)$$

where  $J_{sc}$  is the recorded short-circuit current density for a monochromatic incident power density  $P$  and  $\lambda$  is the wavelength of the incident radiation. Thus for a radiation of 3.5 mW/cm<sup>2</sup> peaking at 363 nm and a current density of 0.085 mA/cm<sup>2</sup>, the IPCE% value was 8.3%.

In the presence of ethanol, the above data changed dramatically. In accordance with the data of Fig. 2, it suffices to add a small quantity of ethanol to get a large variation in both voltage and current. Fig. 4 shows the variation of the short-circuit cur-

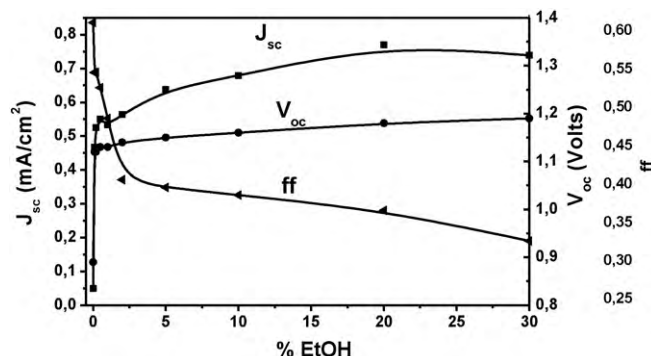


Fig. 4. Variation of the short-circuit current density  $J_{sc}$ , the open-circuit voltage  $V_{oc}$  and the fill factor FF of the cell as a function of ethanol volume percentage in the anode compartment. The values of the actual currents measured can be calculated by multiplying by 12 cm<sup>2</sup> (the surface of the anode electrode).

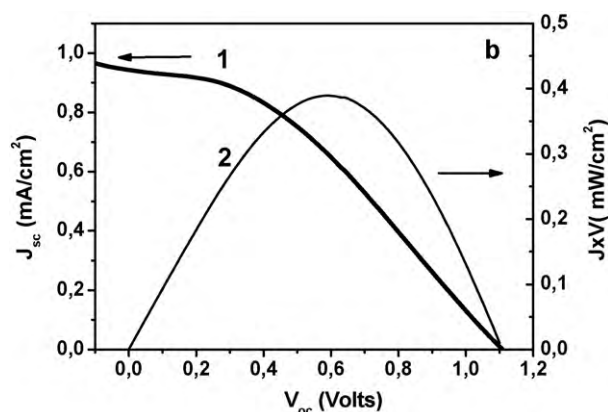


Fig. 5. J-V curve and variation of the  $J \times V$  product for a cell with 20 vol.% EtOH in the anode compartment. The corresponding fill factor was 37%.

rent density, the open-circuit voltage and the FF with respect to ethanol concentration in the electrolyte. Ethanol was only added in the electrolyte of the anode compartment (cf. Fig. 1). Both  $J_{sc}$  and  $V_{oc}$  increased very fast at small ethanol concentrations and then the increase reached saturation. Interestingly, while current and voltage increased, the FF suffered a dramatic decrease at small alcohol additions and continued with a smaller further decrease at larger ethanol concentrations. Obviously, the two-compartment cell of Fig. 1a poorly responds to large current flow demonstrating a small fill factor in that case. Indeed, as can be seen in Fig. 5, showing J-V characteristics, when the ethanol content in the anode compartment was 20 vol.%, despite the improvement in  $J_{sc}$  and  $V_{oc}$ , the FF had a poor shape. The corresponding value of IPCE% in that case for  $J_{sc} = 0.94 \text{ mA/cm}^2$  was 92%.

This high External Quantum Efficiency, more than 10 times higher than in the absence of ethanol, is obviously due to the large increase of current in the presence of the fuel. This efficient conversion of photons into electrons is due to the efficient scavenging of holes in the presence of the fuel. The low fill factor, in spite of the high short-circuit current, is due to the inefficient geometry of the cell. Other configurations, based on larger electrode surface, shorter distance between anode and cathode [41,42], possibly, continuous aeration of the electrolyte (cf. Refs. [27,32]) may improve fill factor. This is a matter of further research, which is been carried on in our laboratory.

The open-circuit voltage  $V_{oc}$  in the presence of ethanol reached values approaching 1.2 V, i.e. more than 0.3 V higher than in the absence of ethanol, as expected and in accordance with the data of Fig. 2. The efficient hole scavenging by ethanol liberates more free electrons, which raise the Fermi level of the semiconductor and make its potential more electronegative, thus increasing the potential difference between anode and cathode and the open-circuit voltage. The advantage then of using a two-compartment cell, among others, is also in the fact that open-circuit potential can be made higher by adding the fuel in the anode compartment.

The J-V curves of Figs. 3–5 were measured on fresh samples. Continuous functioning of the cell for several hours resulted in a slow decrease of both current and voltage. When the quantity of added ethanol was small, decrease was naturally due to alcohol consumption. When alcohol quantity was large, we detected an aldol condensation [43] that also affected results. It seems that practical applications of the present cell will necessitate a design for fast consumption and continuous supply of the fuel to avoid complications. Alcohol diffusion through the frit will also affect the functioning of the cell. A design of a hydroxyl-transporting membrane can take care of this problem. However, these matters are beyond the scope of the present work.

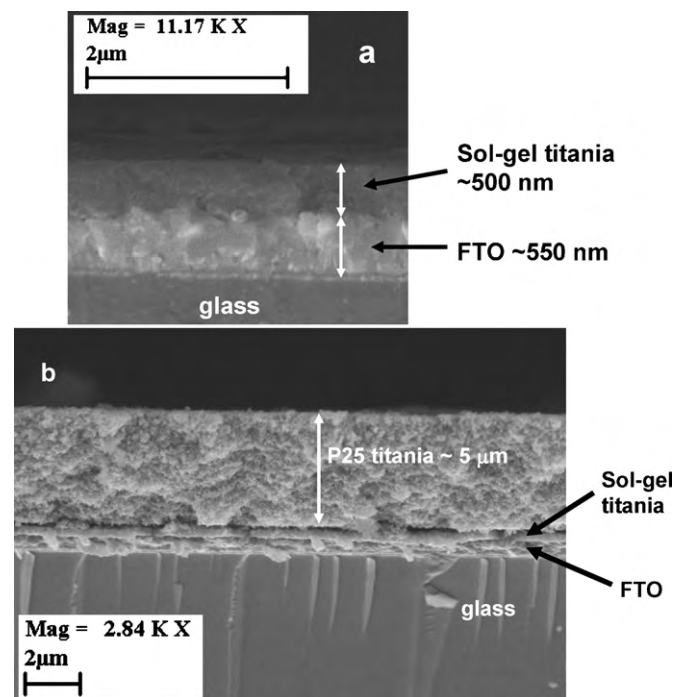
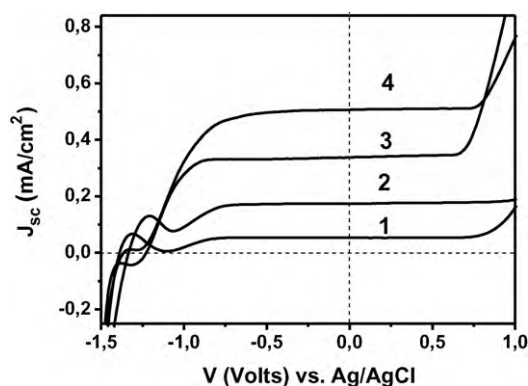


Fig. 6. FESEM cross-sectional image of a sol-gel titania 2-layer film (a) and a combination of sol-gel titania with one layer of P25 titania (b), both deposited on FTO electrodes.

### 3.3. Optimization of the titania film

The above described cell was not optimized. However, several optimization procedures could be undertaken by a variety of approaches. In the present work, we have tried to optimize performance by studying one of the basic parameters of the cell: the structure of the titania film deposited on the anode electrode. As explained in Section 2, besides using commercial Degussa P25, titania can be also deposited as a nanoparticulate film by the sol-gel method, involving Triton X-100 as surfactant template. It has been previously shown [35] that this material makes a compact nanostructure of small anatase nanoparticles of diameter about 6.5 nm. A FESEM cross-sectional view of this 2-layer sol-gel titania (i.e. two dipping and one calcination step) can be seen in Fig. 6a. No boundary was observed between the two layers, which made a uniform film of around 500 nm thick, lying on top of the compact FTO layer of about 550 nm thick. On the contrary, when commercial titania was deposited on top of this sol-gel titania, the boundary between these two materials was easily distinguished, as can be seen in Fig. 6b. One layer of Degussa P25 gave a film with thickness of around 5 μm, as can be seen in Fig. 6b. Several combinations of sol-gel titania and of commercial P25 gave various anode electrodes. By keeping the rest of the reactor the same, both in terms of geometry and materials, a varying behavior was observed. A characteristic example is given in Fig. 7. A 2-layer sol-gel titania alone gave the lowest saturation current density ( $0.05 \text{ mA/cm}^2$ , curve 1 of Fig. 7).

By applying several such 2-layer depositions of sol-gel titania, the film thickness progressively grew and so did the current. We tested anodes with film thickness up to about 2 μm, i.e. about 4 × 2-layer depositions. Beyond that, the coherence of the film was poor and the results not reproducible. The highest saturation current density, obtained with 2 μm sol-gel titania, was  $0.18 \text{ mA/cm}^2$  (curve 2). When a single-layer Degussa P25 film of about 5 μm was used alone (curve 3), the saturation current density was  $0.35 \text{ mA/cm}^2$ . However, when a single-layer titania P25 was deposited on top of a 2-layer sol-gel titania (i.e. the sample



**Fig. 7.** Variation of current density with voltage in a three-electrode single-compartment reactor. Curves 1–4 were recorded under UVA (Black Light) irradiation and correspond to different films of multilayer nanostructured titania made of (1) 2-layer sol–gel titania, (2) 4 × 2-layer sol–gel titania, (3) 2-layer titania Degussa P25, and (4) 2-layer sol–gel titania plus one layer Degussa P25 on the top. All measurements were made in the presence of 5 vol.% ethanol. The electrolyte contained 0.2 M NaOH. The values of the actual currents measured can be calculated by multiplying by 12 cm<sup>2</sup> (the surface of the anode electrode).

of Fig. 6b), a large increase of current density has been observed (0.51 mA/cm<sup>2</sup>, curve 4 of Fig. 7). This optimized behavior is due to the better transport of conduction band electrons to the underlying electrode thanks to the higher conductivity of the compact sol–gel titania layer. This fact is known from applications in Dye-sensitized Solar Cells and Hybrid Oxide-Polymer Solar Cells [35]. If the anode electrode is made of only the compact titania layer, penetration of the electrolyte is limited. If it is made of only the commercial P25 titania, which forms an open structure [35], as can be seen in the FESEM image of Fig. 8, penetration of the electrolyte is extensive but transfer of electrons is less efficient. Combination of the two in a multilayer structure gave an optimum result compromising electrolyte penetration with electron transfer capacity. This is also expressed by the relative values of the fill factor, measured under identical other conditions but with varied anode structure. Table 1 shows these values. It is seen that the compact sol–gel titania gives larger fill factors and this is due to the better electron conducting property of these materials. Thicker sol–gel films gave a lower fill factor than thinner ones, suggesting the importance of the electron transport efficiency from the semiconductor to the underlying electrode. P25 titania by itself gave the lowest fill factor but improvement was achieved in the combined structure (last row). It is then concluded that better results could be obtained with multilayer titania. Of course, it is much easier to make electrodes only with commercial titania, than to follow the tedious procedure

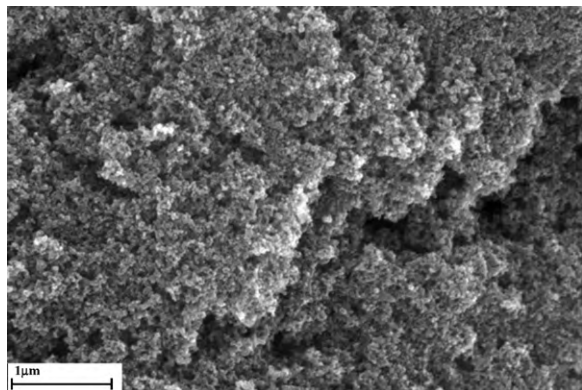


**Fig. 8.** Top FESEM view of the P25 titania film. The material consists of nanoparticles of about 25–30 nm. The size of the bar is 1 μm.

**Table 1**

Values of the fill factor of the two-compartment cell with anode bearing different titania films. Ethanol content 20 vol.%.

Titania film structure	FF
2-Layer sol–gel titania	0.53
4-Layer sol–gel titania	0.46
6-Layer sol–gel titania	0.40
8-Layer sol–gel titania	0.40
1-Layer titania P25	0.28
2-Layer sol–gel titania + 1-layer titania P25	0.31

of the multilayer structure. For this reason, most of the above data were obtained with commercial titania alone.

#### 4. Conclusions

A PhotoFuelCell has been constructed, which photoelectrochemically oxidizes ethanol and produces electricity under UVA excitation (363 nm). The anode was an FTO electrode bearing nanocrystalline titania. The cathode was a carbon cloth bearing a catalytic layer of Carbon Black and Pt. The cell was composed of two compartments separated by a silica frit. Aqueous NaOH electrolyte filled both compartments providing high pH values. The anode compartment also contained the “fuel”, i.e. ethanol. The cell run in the presence of oxygen and functioned according to the model described by reactions (3) and (5). The electric current obtained in the presence of ethanol was much larger than in its absence while the open-circuit voltage increased by about 300 mV in the presence of ethanol and reached 1.2 V. The composition of the titania film is important for the behavior of the cell. Combination of a thin compact layer of sol–gel titania with overlying titania layer made of Degussa P25 gave the highest current. This result is due to the fact that the P25 layer provides an open structure allowing for better electrolyte penetration, at the same time allowing for thick layer deposition with a facile procedure. The underlying layer of compact sol–gel titania facilitates electron transport towards the electrode. The synergy of the two materials had a beneficial effect on cell characteristics. The present work shows that it is possible to efficiently produce electricity by consuming light and an organic waste as fuel.

#### Acknowledgements

The authors are very thankful to Dr.V.Dracopoulos of FORTH-ICEHT Patras for the FESEM data and to Dr.S.Neophytides of FORTH-ICEHT Patras for very helpful discussions concerning this work. Financial support from the E.ON International Research Initiative is gratefully acknowledged. Responsibility for the content of this publication lies with the authors

#### References

- [1] T. Sakata, T. Kawai, Chem. Phys. Lett. 80 (1981) 341.
- [2] M. Barbeni, E. Pelizzetti, E. Borgarello, N. Serpone, M. Gratzel, L. Balducci, M. Visca, Int. J. Hydrogen Energy 10 (1985) 249.
- [3] M. Kawai, T. Kawai, S. Naito, K. Tamaru, Chem. Phys. Lett. 110 (1984) 58.
- [4] G.R. Bamwenda, S. Tsubota, T. Nakamura, M. Haruta, J. Photochem. Photobiol. A: Chem. 89 (1995) 177.
- [5] B. Ohtani, K. Iwai, S.-i. Nishimoto, S. Sato, J. Phys. Chem. B 101 (1997) 3349.
- [6] M. Asshokumar, Int. J. Hydrogen Energy 23 (1998) 427.
- [7] C.M. Blount, J.A. Buchholz, J.L. Falconer, J. Catal. 197 (2001) 303.
- [8] W. Cui, L. Feng, X. Chenghua, S. Lu, F. Qui, Catal. Commun. 5 (2004) 533.
- [9] A.A. Nada, H.A. Hamed, M.H. Barakat, N.R. Mohamed, T.N. Veziroglu, Int. J. Hydrogen Energy 33 (2008) 3264.
- [10] Y. Mizukoshi, Y. Makise, T. Shuto, J. Hu, A. Tominaga, S. Shironita, S. Tanabe, Ultrason. Sonochem. 14 (2007) 387.
- [11] M. Matsuoka, M. Kitano, M. Takeuchi, K. Tsujimaru, M. Anpo, J.M. Thomas, Catal. Today 122 (2007) 51.
- [12] A. Patsoura, D.I. Kondarides, X.E. Verykios, Catal. Today 124 (2007) 94.
- [13] D.I. Kondarides, V.I. Daskalaki, A. Patsoura, X.E. Verykios, Catal. Lett. 122 (2008) 26.

- [14] N. Strataki, V. Bekiari, D.I. Kondarides, P. Lianos, *Appl. Catal. B* 77 (2007) 184.
- [15] N. Strataki, P. Lianos, *J. Adv. Oxid. Technol.* 11 (2008) 111.
- [16] P. Lianos, N. Strataki, M. Antoniadou, *Pure Appl. Chem.* 81 (2009) 1441.
- [17] H. Fujishima, K. Honda, *Nature* 298 (1972) 37.
- [18] J.G. Mavroides, D.I. Tchernev, J.A. Kafalas, D.F. Kolesar, *Mat. Res. Bull.* 10 (1975) 1023.
- [19] F. Chojnowski, P. Clechet, J.-R. Martin, *Chem. Phys. Lett.* 84 (1981) 555.
- [20] N. Getoff, *Int. J. Hydrogen Energy* 15 (1990) 407.
- [21] T. Ohno, S. Izumi, K. Fujihara, Y. Masaki, M. Matsumura, *J. Phys. Chem. B* 104 (2000) 6801.
- [22] T. Bak, J. Nowotny, C.C. Sorrell, *Int. J. Hydrogen Energy* 27 (2002) 991.
- [23] J.H. Park, S. Kim, A.J. Bard, *Nanoletters* 6 (2006) 24.
- [24] S.K. Mohapatra, M. Misra, K. Mahajan, S. Raja, *J. Phys. Chem. C* 111 (2007) 8677.
- [25] P.V. Kamat, *J. Phys. Chem. C* 111 (2007) 2834.
- [26] M. Kaneko, H. Ueno, K. Ohnuki, M. Horikawa, R. Saito, J. Nemoto, *Biosens. Bioelectron.* 23 (2007) 140.
- [27] M. Kaneko, H. Ueno, R. Saito, S. Yamaguchi, Y. Fujii, J. Nemoto, *Appl. Catal. B* 91 (2009) 254.
- [28] M. Antoniadou, P. Lianos, *J. Photochem. Photobiol. A: Chem.* 24 (2009) 69.
- [29] M. Antoniadou, P. Lianos, *Catal. Today* 144 (2009) 166.
- [30] M. Kaneko, J. Nemoto, H. Ueno, N. Gokan, K. Ohnuki, M. Horikawa, R. Saito, T. Shibata, *Electrochem. Commun.* 8 (2006) 336.
- [31] M. Antoniadou, D.I. Kondarides, D. Labou, S. Neophytides, P. Lianos, *Sol. Energy Mater. Solar Cells* 94 (2010) 592.
- [32] H. Ueno, J. Nemoto, K. Ohnuki, M. Horikawa, M. Hoshino, M. Kaneko, *J. Appl. Electrochem.* 39 (2009) 1897.
- [33] M. Antoniadou, P. Bouras, N. Strataki, P. Lianos, *Int. J. Hydrogen Energy* 33 (2008) 5045.
- [34] S. Ito, P. Chen, P. Comte, M.K. Nazeeruddin, P. Liska, P. Pechy, M. Gratzel, *Prog. Photovolt.: Res. Appl.* 15 (2007) 603.
- [35] M. Antoniadou, E. Stathatos, N. Boukos, A. Stefopoulos, J. Kallitsis, F.C. Krebs, P. Lianos, *Nanotechnology* 20 (2009), Art. No. 495201.
- [36] S.R. Morrison, T. Freund, *J. Chem. Phys.* 47 (1967) 1543.
- [37] M. Miyake, H. Yoneyama, H. Tamura, *Chem. Lett.* (1976) 635.
- [38] O.K. Varghese, C.A. Grimes, *Solar Energy Mater. Solar Cells* 92 (2008) 374.
- [39] M. Zhou, N.R. de Tacconi, K. Rajeshwar, *J. Electroanal. Chem.* 421 (1997) 111.
- [40] N.R. de Tacconi, H. Wenren, D. MacChesney, K. Rajeshwar, *Langmuir* 14 (1998) 2933.
- [41] K. Drew, G. Girishkumar, K. Vinodgopal, P.V. Kamat, *J. Phys. Chem. B* 109 (2005) 11851.
- [42] B. Seger, P.V. Kamat, *J. Phys. Chem. C* 113 (2009) 18946.
- [43] M. Antoniadou, D.I. Kondarides, P. Lianos, *Catal. Lett.* 129 (2009) 344.